Trans Indian Inst Met (2018) 71(12):3103–3110
https://doi.org/10.1007/s12666-018-1501-y

TECHNICAL PAPER

A Comparative Study on Direct and Pulsed Current Micro-plasma Arc Welding of Alloy Ti–6Al–4V

Amirkeyvan Rahimi[1] · Morteza Shamanian[1] · Ahmadreza Rahimi[1] · Jalal Kangazian[1]

Received: 15 December 2017 / Accepted: 5 November 2018 / Published online: 19 November 2018
© The Indian Institute of Metals - IIM 2018

Abstract In this project, the sheet of Ti–6Al–4V alloy (annealed) with a thickness of 1 mm was welded with butt joints by means of pulsed current micro-plasma arc welding without using a filler metal. The purpose of this study is to optimize parameters in the event of increasing tensile strength by using pulse current and its comparison with the pulse-free system. Optical microscope and scanning electron microscope were used to investigate the type of phases, microstructure of weld metal, base metal and heat-affected zone. Results illustrated that due to the low thickness of the sheet, the non-use of filler metal in the welding process and the lower heat input of this process, all contributed to a higher cooling rate of the molten pool.

Keywords Pulsed current micro-plasma arc welding · Tensile strength · Ti–6Al–4V alloy

1 Introduction

Due to its high specific strength and stiffness and its inherently good corrosion resistance, Ti–6Al–4V as alpha (α) + beta (β) titanium alloy is widely used in aerospace, marine and surgical implants. The choice of the bonding method of this alloy and its parameters has always played a significant role in determining the mechanical properties of the weld metal. In general, in arc welding processes such as gas tungsten arc welding (GTAW) and plasma arc welding (PAW), there is a large heat input that causes an increase in the size of the grain of the initial beta phase in the weld metal region [1–4] during freezing. The process of plasma welding at a low current level, which is about 0.06–50 Amp, is called micro-plasma welding. In the micro-plasma process, the heat required to weld the metals is provided by an electric arc between the workpiece and the tungsten electrode. The micro-plasma welding process produces a cylindrical arc, which produces an infiltrated weld. Pulse current system can be used to reduce the size of the β-phase grain of Ti–6Al–4V and to minimize the martensite phase because in addition to reducing the area of the under current and time chart, which results in lower heat input to the workpiece, it results in less warp of the workpiece compared to the pulse-free system. However, weldability of Ti–6Al–4V is poor [1, 5] because of the formation of acicular hard martensite and a large prior beta (β) grain size in the fusion zone (FZ) which leads to a low ductility [1, 6–8].

Rao et al. [9] showed that the control of heat input had an influence on grain size, microstructure and mechanical properties. Kishore et al. [10] showed that pulsed current system was responsible for refinement of prior grains, which resulted in a high hardness and high tensile strength of the weldment. Chen et al. [11] demonstrated the dynamically controlled plasma arc welding process to weld Ti–6Al–4V alloys. They showed that the process reduced the heat input which resulted in a reduction grain size without increasing the acicular microstructure.

In this research, pulsed micro-plasma arc method is used to weld the thin sheet of Ti–6Al–4V alloy. The purpose of this study is to optimize the parameters in the event of increasing tensile strength by using pulse currents and its comparison with the pulse-free system. I_p (peak current), t_p (time of peak current), I_b (background current) and t_b (time

✉ Amirkeyvan Rahimi
r.rahimi7075@gmail.com

[1] Department of Materials Engineering, Isfahan University of Technology, Isfahan 8415683111, Iran

Table 1 Chemical composition of Ti–6Al–4V alloy (wt%)

Element	Al	V	Fe	C	N	O	H	Ti
Amount (wt%)	6.1	3.9	0.25	0.08	0.05	0.2	0.009	Bal.

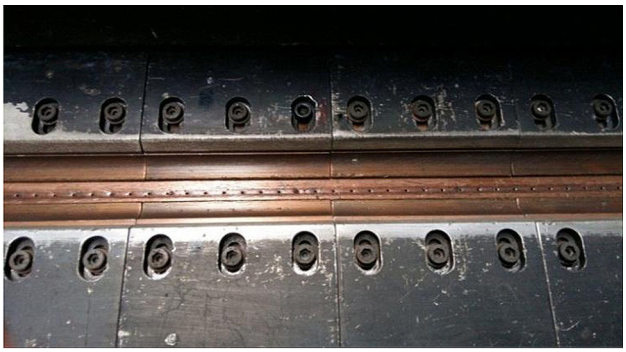

Fig. 1 Pneumatic Feronus fixture on the Magic Wave 2600 device

Table 2 Gas flow rate in the process of micro-plasma arc welding

Protective gases	Flow rate (L/min)
Micro-plasma shielding gas	0.3
Shielding gas	8
Backing gas	15
Leading gas	12
Trailing gas	12

Table 3 Parameters of the MPAW process

Sample	I_p (A)	I_b (A)	t_p (s)	t_b (s)	$(I_b/I_p) \times 100$ (%)
P_1	48	12	0.25	0.25	25
P_2	40	20	0.25	0.25	50
P_3	34	26	0.25	0.25	75
P_4	30	30	0.25	0.25	100

of background current) are the most important parameters in this study.

2 Experimental Procedure

In this research, the sheet of Ti–6Al–4V alloy (annealed) with a thickness of 1 mm was welded. The chemical composition of the Ti–6Al–4V alloy is presented in Table 1. To clean the base metal before welding, the samples were degreased by methyl ethyl ketone, and then, they were washed with water. In order to remove the oxide surface, the samples were placed in a solution containing 40% nitric acid, 4% fluorhidrico acid and 56% water [12] and left in the environment temperature for 20–30 min. Then, they were washed with water and dried. According to Fig. 1, open-hearth fixture method was used in order to protect the roots of the weld and surroundings of the molten area and to prevent the warping of the samples. Plasma Fix 50S (micro-plasma system) was used to weld the sheet of Ti–6Al–4V. The frequency of the device was 50 Hz, the voltage was 9–9.2 V, and the welding speed was 11 cm/min. The temperature of the samples before the welding was about 25 °C. In order to provide a neutral atmosphere, argon gas with 99.998% purity was used as shielding, trailing, leading and backing gases. The gas flow rates are given in Table 2. The gas was applied for 5 and 20 s before applying the arc[1] and after applying the arc,[2] respectively, to clean and protect the molten pool.

Figure 1 shows the pneumatic Feronus fixture with a copper backing installed on a fully automatic linear machine with the maximum jaw pressure of about 12 bars. In this study, the used pressure was 4 bars. After preparing the samples and placing them in the bracket, they were welded with butt joints by means of micro-plasma arc welding (MPAW) without using a filler metal. The polarity was pulsed current electrode negative or PDCEN using tungsten electrode containing two percent thorium oxide (red) having a diameter of 1.6 mm and a vertex angle of 40–45. The diameter of the copper nozzle was 1.2 mm, and it was controlled during the welding process.

According to Table 3, the samples were welded with different current ratios (I_b/I_p) and with the same time ratio (t_b/t_p). The average current for all welding samples was 30 Amp; therefore, the heat input of all MPAW samples was equal, and just the difference was in the I_b/I_p ratio. To examine the micro-hardness, Vickers method was used with a force of 100 g and at intervals of 500 mm in 35 s. According to Fig. 2, samples were prepared from transverse section of the weld area of a length of 10 cm and a width of 1 cm in accordance with the standards of ASTM E8, A370; the tensile test was carried out with a crosshead velocity of 1 mm/min at ambient temperature. In order to study the microstructure, samples were polished using 80, 120, 600, 1200, 2400 SiC papers, and then, for etching Kroll solution containing 3 cc HF, 10 cc HNO_3, 100 cc H_2O was used at 25 °C for 10 s. The Image J software was used for estimation of grain size.

3 Results and Discussion

3.1 Weld Metal Structure

According to Fig. 3 and Table 4, by increasing I_b/I_p, the volume of the weld metal and weld width of the sample

[1] Pre-gas.

[2] Post-gas.

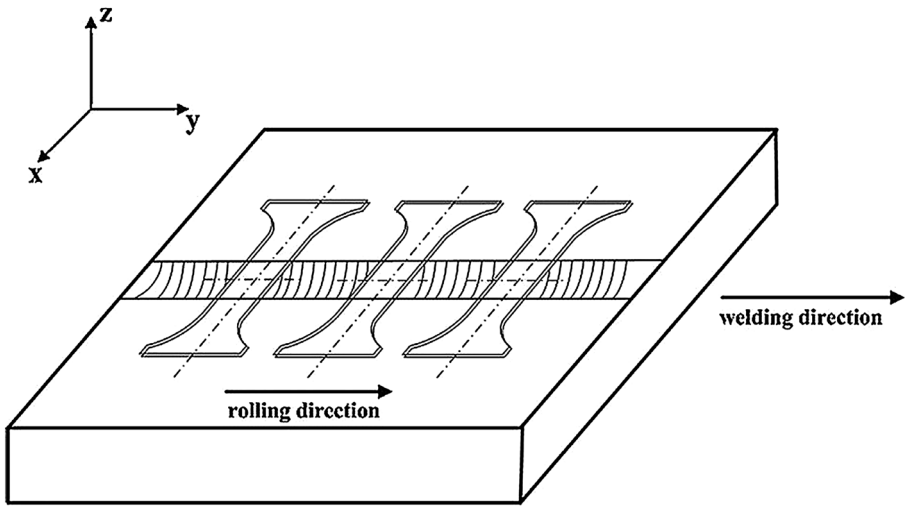

Fig. 2 Sketch map of specimens' preparation

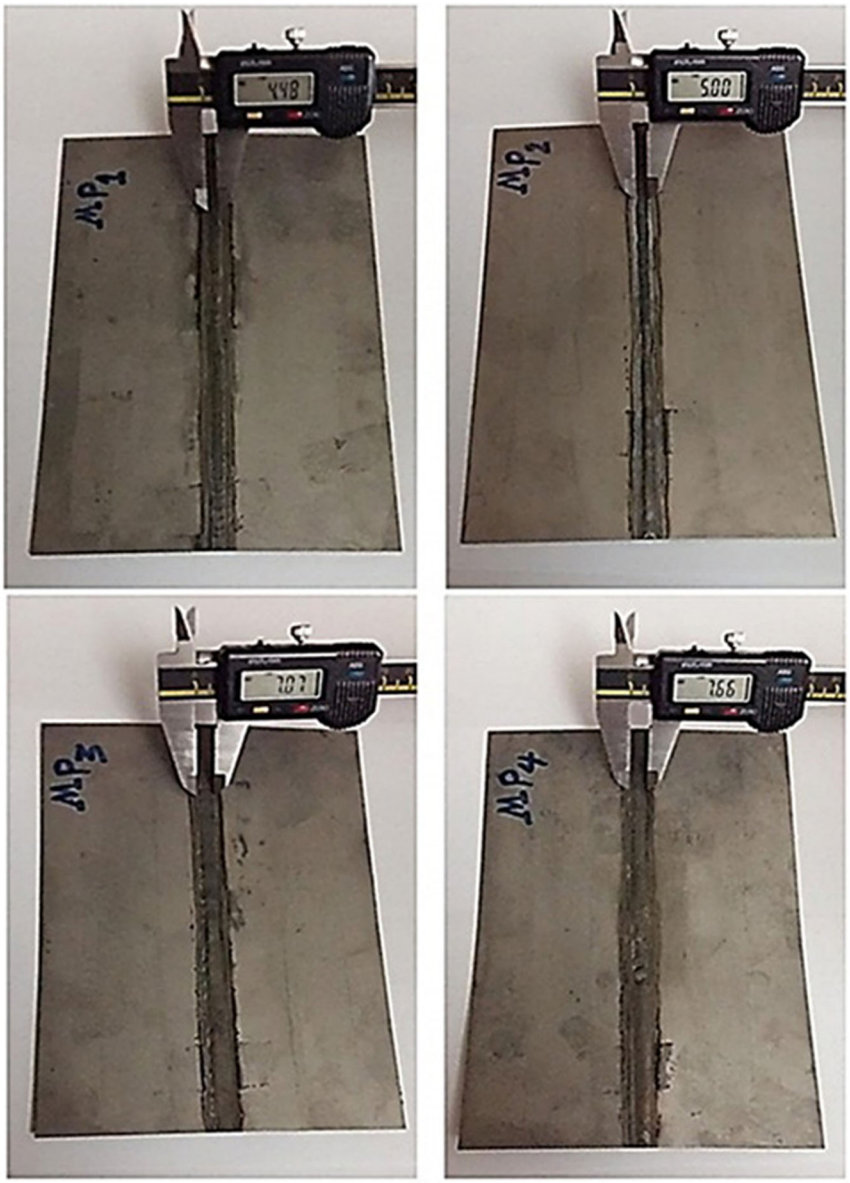

Fig. 3 Weld width of specimens measured by a caliper

Table 4 Weld width of the specimens

Code	Weld width (mm)
P_1	4.48
P_2	5
P_3	7.07
P_4	7.66

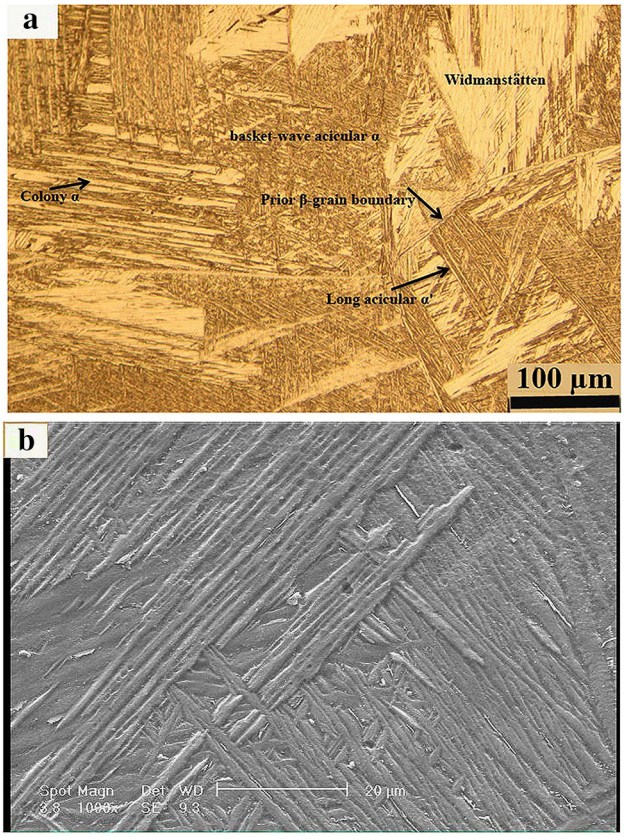

Fig. 4 Microstructure of the weld metal of the P_1 sample, **a** optical microscope (OM) image and **b** scanning electron microscope (SEM) image

increases, due to the increase in the base current (I_b) and due to fusion. High I_p in the welding process, which create a lot of heat in the joint of the P_1 sample, results in increase in the volume of the weld metal. However, when the welding current is placed in the I_b cycle, the melting stops and only the welding arc is stable; and because of the low background current and absence of fusion, the volume of the weld metal is reduced, and therefore, the weld width is less than other specimens. According to Fig. 4, values of fine structure of the α layer alongside the β-layer phase (Widmanstätten structure) with large amounts of acicular α with long branches on the edge of the fusion zone causes the structure of the weld metal to become extremely brittle; therefore, it has the least tensile strength among the

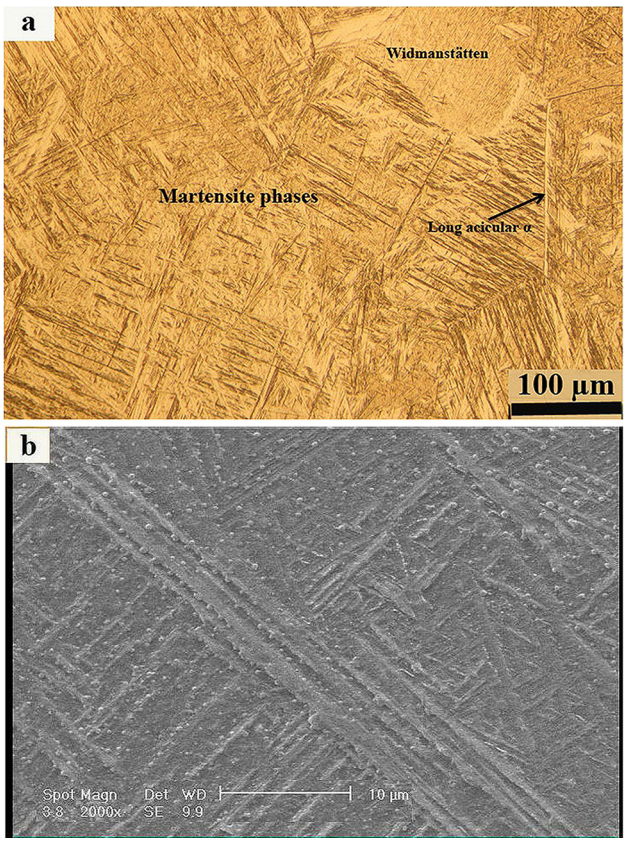

Fig. 5 Microstructure of the weld metal of the P_2 sample, **a** OM image and **b** SEM image

samples, but often short branches are seen as a basket-wave acicular α in the middle of the weld metal.

In the P_2 sample, due to less I_p, less heat is generated in the joint. Moreover, when the welding current is I_b, the melting process is slow enough which results in a slight increase in the weld width. According to Fig. 5, by comparing the P_2 sample with P_1, the volume of the weld metal is found to be slightly higher, but it has a higher cooling rate. This results in a reduction in the amount of the α-phase-type Widmanstätten and an increase in the amount of martensite phases with little amount of acicular α. Thus, the flexibility is reduced, and the hardness and strength of the weld metal are increased.

In P_3 sample, due to less I_p (34 Amp), less heat is produced in the joint, but when the I_b welding current (26 Amp) is applied, the melting of the base metal in the half cycle of the I_b increases sharply. This results in an increase in the heat generated in the joint and a significant increase in the weld width of the sample. According to Fig. 6, in the region of the weld metal, due to the increase in the volume of molten metal and the reduction in the rate of cooling, a structure with a lower degree of martensite phase is obtained which results in a slight reduction in the hardness and strength of P_3 compared to the P_2 specimen.

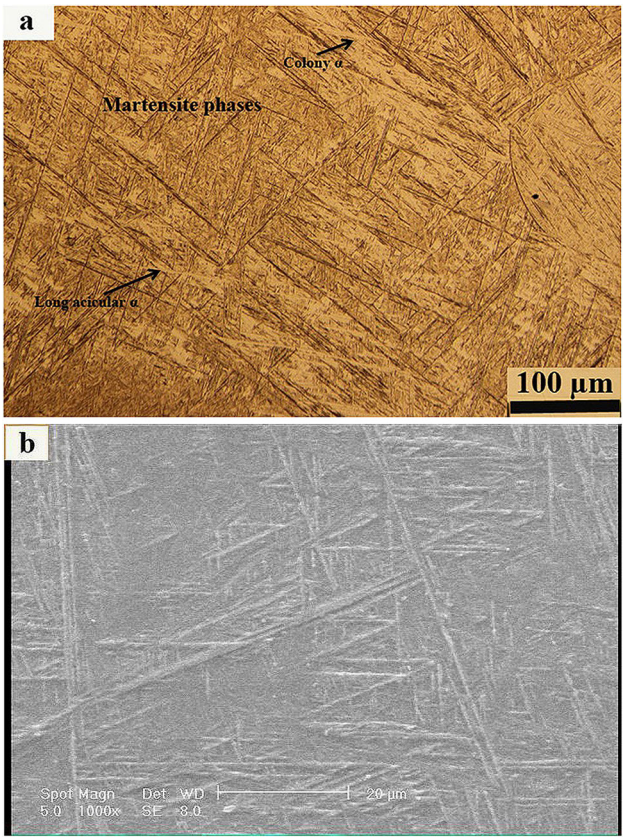

Fig. 6 Microstructure of the weld metal of the P_3 sample, **a** OM image and **b** SEM image

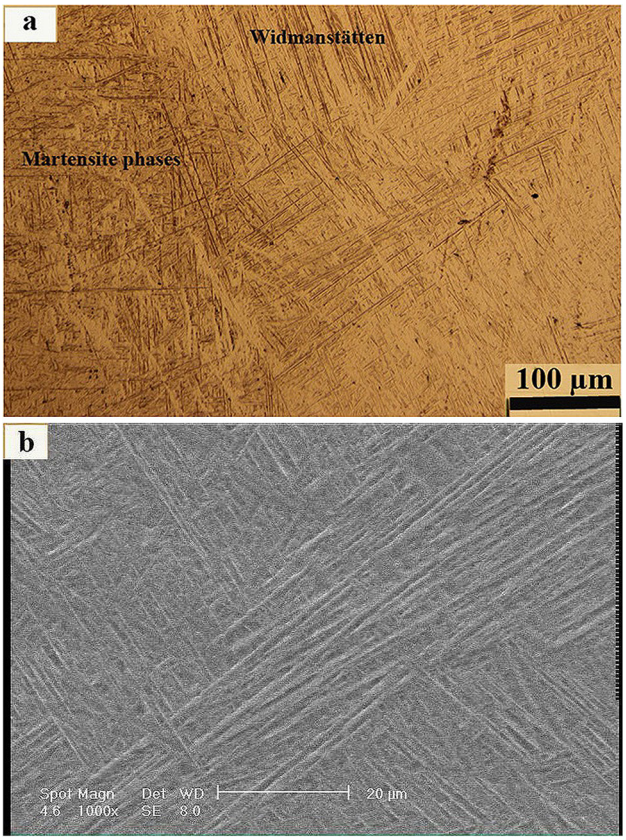

Fig. 7 Microstructure of the weld metal of the P_4 sample, **a** OM image and **b** SEM image

In P_4 sample, the pulse-free current system (30 Amp) is used in welding. Therefore, the volume of the molten metal increases, and the cooling rate in the fusion zone is reduced. A comparison of the P_4 sample with the previous specimens shows that due to the lack of pulsed current, the volume of the weld metal increases and it has the lowest cooling rate in the fusion zone after the P_1 sample. According to Fig. 7, it results in an increase in fine-layer α structure and acicular α and a decrease in martensite phases in the weld metal.

3.2 Heat-Affected Zone Structure

According to Fig. 8, due to high peak current of the P_1 sample, a large amount of heat produces the molten pool and so the cooling rate at the heat-affected zone is reduced compared to other samples. Therefore, in this area, martensite transformation does not take place and the α-phase grains often grow in a delicate column. In the adjacent region of the base metal, the growth of phase α grains is fine.

In the P_2 sample, due to lower peak current, the amount of heat applied to the heat-affected zone is less than P_1 sample, which results in a higher cooling rate in this area and the formation of the fine basket-wave α′ with proper distribution, thus significantly improving the mechanical properties of the zone. In P_3 sample, due to the increase in the base current, the heat-affected zone expands and the cooling rate in this zone is lower than in P_2 sample, which causes a coarser basket-wave α′ phase. In P_4 sample, due to the absence of pulsed current, the molten metal volume is higher than other samples; therefore, more heat is transferred to the adjacent region of the molten metal, which reduces the cooling rate in this area. By comparing P_4 sample with other micro-plasma samples, it is observed that it has the coarsest structure of the basket-wave α′ phase that will reduce its mechanical properties relative to other specimens.

3.3 Mechanical Properties

Due to the fact that all micro-plasma specimens are cracked from the weld metal region during tensile tests, the tensile test results show the behavior of the weld metal region. Figures 9 and 10 shows the microhardness profiles of the samples. According to Fig. 11 and Table 5, we can find the relation between the average hardness of the weld

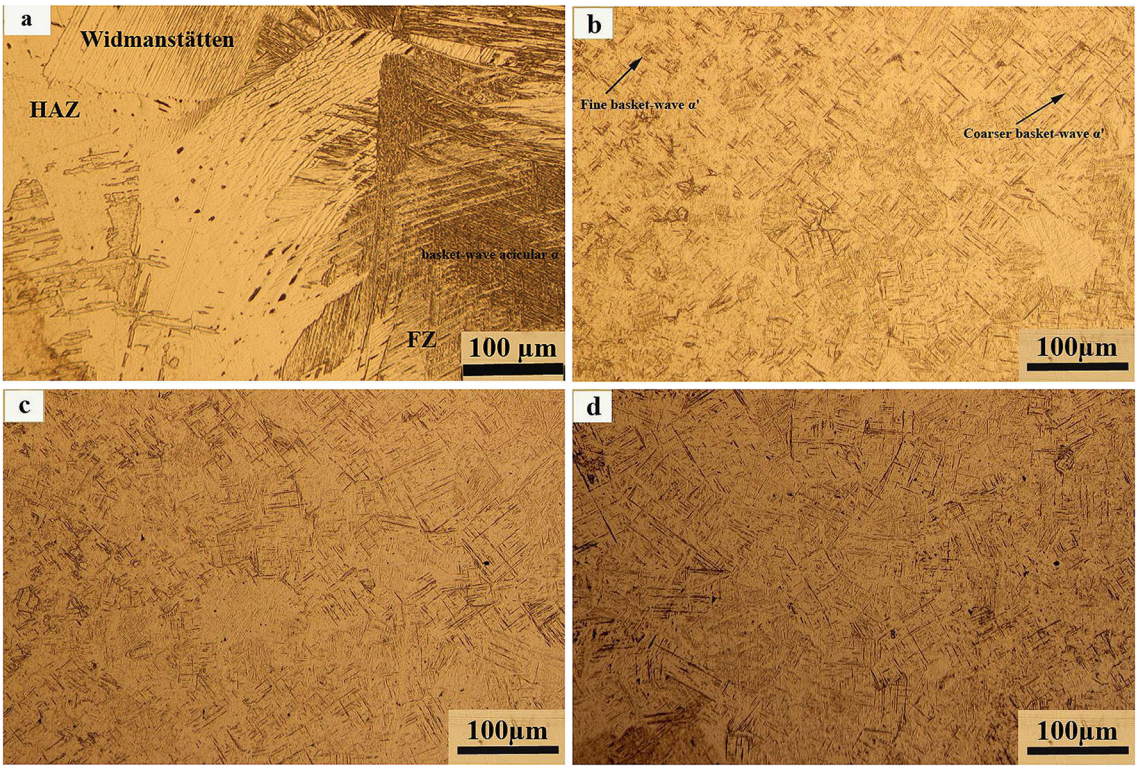

Fig. 8 Microstructure of the heat-affected zone of the specimens, **a** P_1 sample, **b** P_2 sample, **c** P_3 sample and **d** P_4 sample

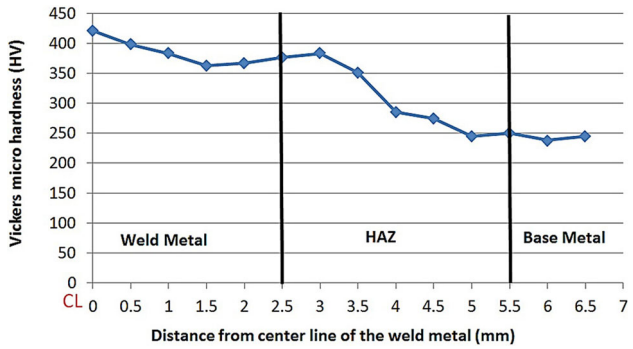

Fig. 9 Microhardness profile of P_2 sample

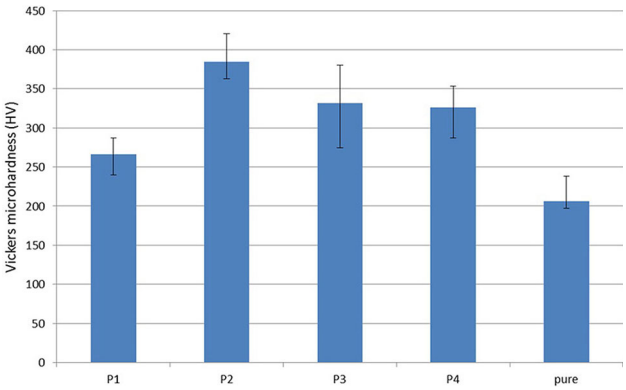

Fig. 11 Average hardness of the weld metal of the specimens

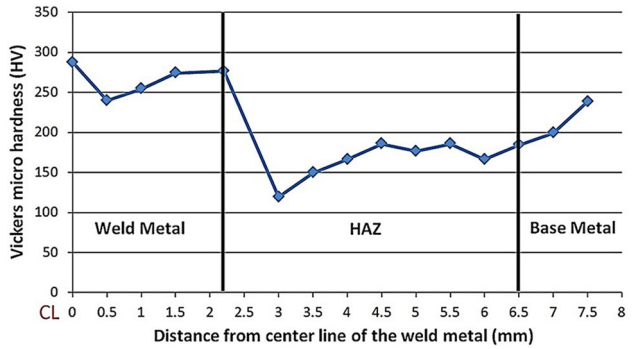

Fig. 10 Microhardness profile of P_1 sample

metal and the results of their tensile strength. The P_2 sample with the highest average hardness (384 HV) and the lowest average grain size (230 µm) in the weld zone has the highest tensile strength (about 90% of base metal strength is acceptable for welding strength). P_3 and P_4 samples with near-average hardness and the grain size of 275 µm and 369 µm, respectively, have close proximity tensile strengths (about 80% of base metal strength is acceptable for welding strength). The P_1 specimen with the lowest average hardness (266 HV) and the highest grain size (413 µm) has the lowest value of tensile strength (494 MPa) among the micro-plasma samples.

Table 5 Mechanical properties and grain size of the fusion zone

Sample	Yield strength (MPa)	Ultimate tensile strength (MPa)	%EL	Grain size (μm)
P_1	494	494	3.6	413
P_2	901	901	2.8	230
P_3	780	780	2.8	275
P_4	775	775	4.7	369
Base metal	1020	1040	16.8	–

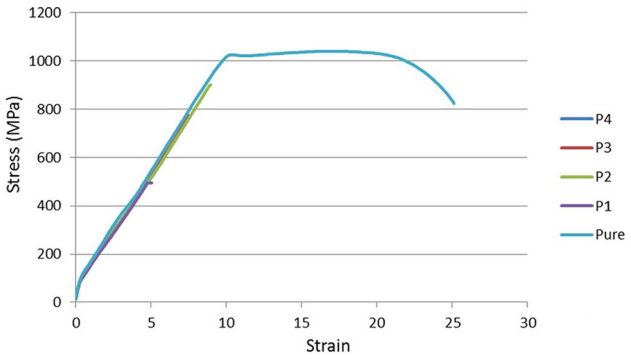

Fig. 12 Stress–strain diagrams of micro-plasma specimens

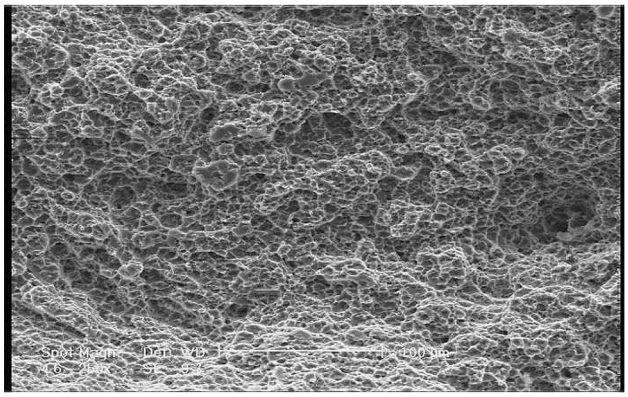

Fig. 13 SEM image of the fracture surface of the Ti–6Al–4V alloy base metal

The Ti–6Al–4V alloy has a low thermal conductivity, and its grain size at the weld metal is very coarse. Using the pulsed current with an optimal ratio causes a decrease in the grain size of the weld metal, which results in the improvement of hardness and tensile strength of the weldment. However, it does not help in increasing the ductility owing to the presence of acicular martensite phase which has a hard and brittle nature. It is the main reason behind decrease in the elongation of weldments in comparison with the original base metal, as shown in Table 5.

According to Table 5 and Fig. 12, in addition to the tension caused by the martensite transformation in the fusion zone, the presence of martensite phase and the residual stresses, caused by the rapid cooling, results in the absence of plastic deformation region in the stress–strain curves of these samples and, hence, a brittle fracture in the weld metal and low toughness are observed.

3.4 Fractography

Figure 13 shows the ductile mode of fracture at the Ti–6Al–4V alloy base metal during tensile test. The presence of fine dimples is in accordance with the highest strength and elongation. As mentioned above, the formation of the hard martensite phase and the brittle acicular phase in the weld metal of micro-plasma samples is observed and it causes the initiation and growth of cracks. In addition, due to the brittleness of the phases, the strength and hardness are greatly increased and the toughness is greatly reduced. According to Fig. 14, for all the micro-plasma samples, brittle fracture mode and cleavage facets are observed along the direction of the hard martensite phases in the fusion zone, and the fracture surface images indicate the sections of martensite phases.

4 Conclusions

The following conclusions can be made:

- The low thickness of the sheet, the non-use of filler metal in the welding process and lower heat input of pulsed current micro-plasma arc welding (PCMPAW) process, all contribute to a higher cooling rate of the molten pool. Consequently, these reduce the amount of soft phases and increase the amount of martensite and acicular α phases in the weld metal region. These phases are susceptible to initiation and crack growth during tensile test, which causes a brittle fracture in the weld metal region with low toughness.
- Samples with the lowest current ratio (I_b/I_p) and high peak current produce high heat in the molten pool, which has the lowest cooling rate of the weld metal among the samples. This is observed as a result of the lowest average hardness. In addition, with the increase in the current ratio I_b/I_p, the weld width increases and

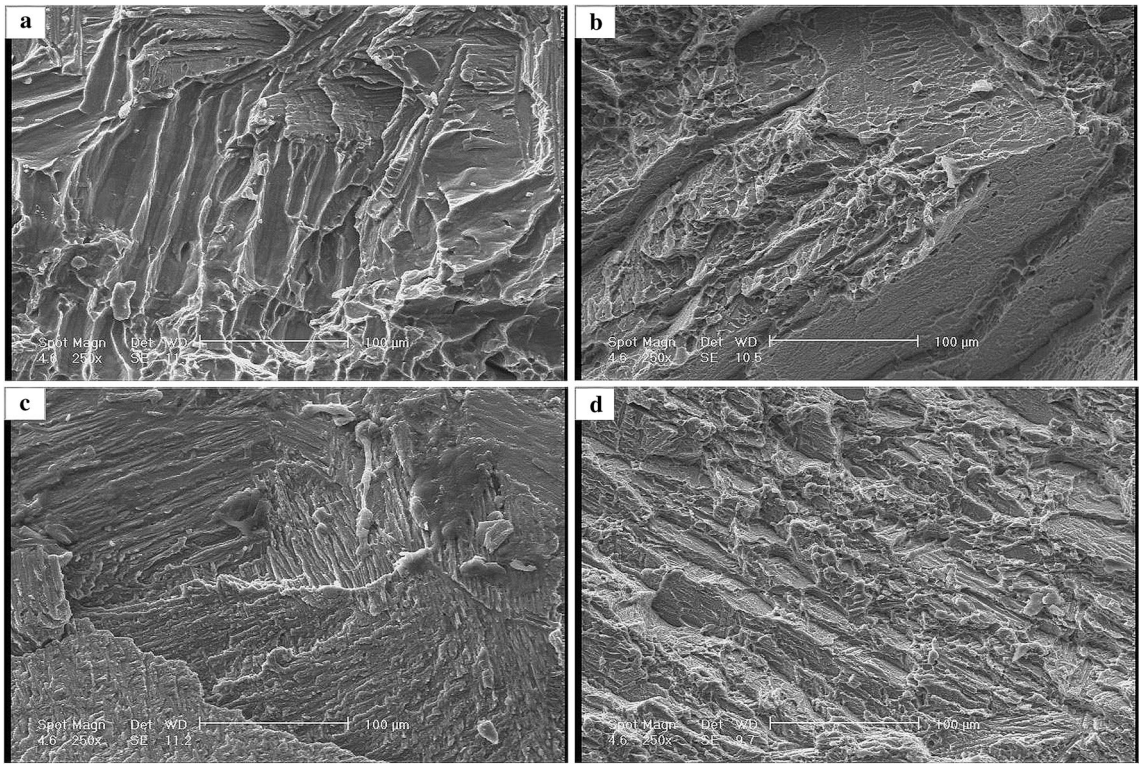

Fig. 14 SEM images of the fracture surface of **a** P_1 sample, **b** P_2 sample, **c** P_3 sample and **d** P_4 sample

the cooling rate decreases, which reduces the tensile strength and average hardness of the weld metal.

References

1. Cheng D H, *Trans China Weld Inst* **30** (2009) 103.
2. Kumar A, Sapp M, Vincelli J, and Gupta M C, *J Mater Process Technol* **210** (2010) 64.
3. Lin Y C, and Lin Y C, *J Coat Technol Res* **8** (2011) 247.
4. Rokhlin S I, and Guu A C, *Weld J* **72** (1993) 381.
5. Yuan B G, Li C F, Yu H P, and Sun D L, *Trans Nonferrous Metals Soc China* **19** (2009) 423.
6. Zhao H, Han Z, and Chen X F, *Trans China Weld Inst* **26** (2005) 78.
7. Mohandas T, Banerjee D, and Kutumba Rao V V, *Metall Mater Trans A* **30** (1999) 789.
8. Wu K C, *Weld J* **60** (1981) 219.
9. Rao K P, Angamuthu K, and Bala Srinivasan P, *J Mater Process Technol* **199** (2008) 185.
10. Kishore B N, Ganesh S R S, Mythili R, and Saroja S, *Mater Charact* **58** (2007) 581.
11. Chen J, and Pan C, *Trans Nonferrous Metals Soc China* **21** (2011) 1506.
12. Beaslack W A, *Selection and Weldability of Conventional Titanium Alloys*, Vol. 6. ASM Handbook, Metals Park (1992), p 507.